Наносистеми, наноматеріали, нанотехнології
Nanosistemi, Nanomateriali, Nanotehnologii
2025, т. 23, № 1, сс. 101–108
https://doi.org/10.15407/nnn.23.01.0101

PACS numbers: 61.72.Ff, 61.72.Mm, 68.37.Ps, 68.55.J-, 78.20.Ci, 78.66.Li, 81.15.Cd

Light Dispersion in Thin Films of $ZnGa_2O_4:Cr^{3+}$ and $ZnGa_2O_4:Mn^{2+}$ Obtained by RF Ion-Plasma Sputtering

O. M. Bordun[1], I. I. Medvid[1], I. Yo. Kukharskyy[1], V. G. Bihday[1], I. O. Bordun[1], I. M. Kofliuk[1], Zh. Ya. Tsapovska[1], and D. S. Leonov[2]

[1]*Ivan Franko National University of Lviv,*
50, Drahomanov Str.,
UA-79005 Lviv, Ukraine
[2]*Technical Centre, N.A.S. of Ukraine,*
13, Pokrovska Str.,
UA-04070 Kyiv, Ukraine

Thin films of $ZnGa_2O_4:Cr^{3+}$ and $ZnGa_2O_4:Mn^{2+}$ are obtained by high-frequency (RF) ion-plasma sputtering in an argon atmosphere. The surface morphology is studied by AFM, and the sizes of nanocrystallites forming the films are analysed. Based on the interference technique, the refractive index is determined. As found, in films of both types in the visible region, a normal dispersion of the refractive index is observed. The analysis of the single-oscillator three-parameter model used to describe the dispersion dependence is carried out, and the static refractive index n_0, the characteristic energy E_0, the approximation parameter A, and the plasma-oscillations' energy for valence electrons $h\nu_p$ are determined.

Методом високочастотного (ВЧ) йонно-плазмового розпорошення в атмосфері арґону одержано тонкі плівки $ZnGa_2O_4:Cr^{3+}$ і $ZnGa_2O_4:Mn^{2+}$. Методом АСМ проведено дослідження морфології поверхні та проаналізовано розміри нанокристалітів, які формують одержані плівки. На основі інтерференційної методики проведено визначення величини показника заломлення та встановлено, що в плівках обох типів у видимій області спостерігається нормальна дисперсія показника заломлення. Проведено аналізу одноосциляторного трипараметричного моделю, котрого було використано для опису дисперсійної залежности, та визначено статичний показник заломлення n_0, характеристичну енергію E_0, параметер апроксимації A й енергію плазмових коливань для валентних електронів $h\nu_p$.

Key words: zinc gallate, thin films, RF sputtering, surface morphology, refractive index dispersion.

Ключові слова: ґалат Цинку, тонкі плівки, високочастотне напорошення, морфологія поверхні, дисперсія показника заломлення.

(Received 10 February, 2025)

1. INTRODUCTION

$ZnGa_2O_4$-based thin films are promising materials for practical applications in optoelectronics and instrumentation. Due to their optical, dielectric, and performance characteristics, both nominally pure and activated $ZnGa_2O_4$ thin films are used in electron-optical devices, vacuum fluorescent and field emission displays, and gas sensors [1–10].

In general, the optical and electrical properties of thin films are determined by the preparation methods, deposition modes, the presence of heat treatment in different environments, and the introduction of impurities that can change the properties of thin oxide films in the desired direction. In this work, we studied $ZnGa_2O_4$:Cr and $ZnGa_2O_4$:Mn thin films prepared by the RF ion-plasma sputtering method, which is considered optimal for the deposition of multicomponent semiconductor and dielectric films [11].

The study of the optical properties of such films, including the dispersion properties and their relation to the energy structure and crystal-chemical properties, seems relevant. This is because they are used to illuminate optical parts, manufacture optical light filters, or create luminescent screens. The value of the refractive index determines the reflective properties of films, and, accordingly, the dispersion properties determine their spectral distribution.

2. EXPERIMENTAL TECHNIQUE

Thin films of $ZnGa_2O_4$ activated with Cr^{3+} and Mn^{2+} ions with a thickness of 0.3–1 μm were obtained by RF ion-plasma sputtering in an argon atmosphere on amorphous substrates of fused quartz υ-SiO_2. The starting material for the target was a mixture of ZnO and Ga_2O_3 oxides of stoichiometric composition (purity 99.99%). The activator concentration of Cr^{3+} and Mn^{2+} was of 1 mol.%.

The phase composition and structure of the obtained thin films were studied by x-ray diffraction analysis (Shimadzu XDR-600). X-ray diffraction studies have shown the presence of a polycrystalline structure with a predominant orientation in the (002), (113), (004), and (333) planes. The diffractograms and their analysis are described in more detail in [12]. All diffraction maxima are identified according to the selection rules and belong to the $Fd3m$ space

group. This indicates the cubic structure of the obtained films.

The surface morphology of the obtained thin films was studied using an 'Integra TS-150' atomic force microscope (AFM).

The optical transmittance spectra of the thin films were measured on a CM 2203 spectrofluorimeter with a Hamamatsu R928 measuring head. Spectrophotometric techniques are the most common for determining the refractive index n, absorption coefficient, and film thickness h in semiconductor and dielectric films. The technique of Ref. [13] is quite often used, and we used it to determine the optical parameters of $ZnGa_2O_4$:Cr and $ZnGa_2O_4$:Mn thin films.

3. RESULTS AND DISCUSSION

The surface morphologies of $ZnGa_2O_4$:Cr and $ZnGa_2O_4$:Mn thin films were studied by AFM. Characteristic micrographs of the surface of freshly deposited thin films are shown in Fig. 1.

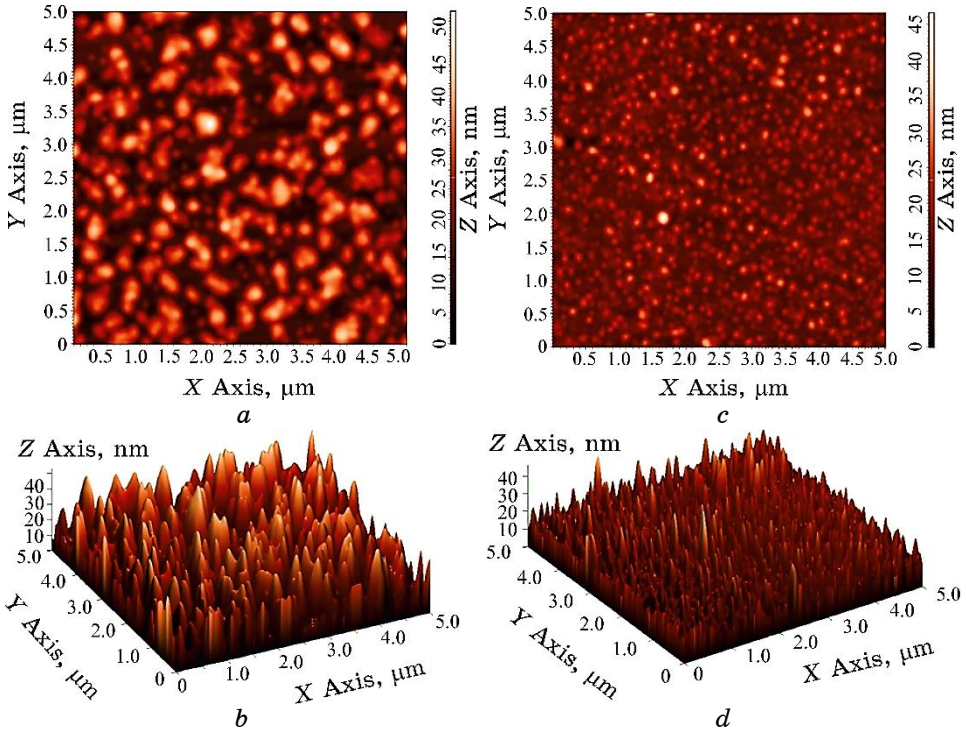

Fig. 1. Images of the surface morphology of freshly deposited $ZnGa_2O_4$:Cr (*a*, *b*) and $ZnGa_2O_4$:Mn (*c*, *d*) thin films. Images *a* and *c* are two-dimensional, *b* and *d* are three-dimensional.

The surface topography of the samples was analysed based on standard parameters listed in Table 1. These values were calculated based on AFM images for areas on the surface of the films of the same size 5000×5000 nm.

The obtained results show that the formation of the structure of $ZnGa_2O_4$:Cr thin films occurs from significantly larger nanocrystallites, the average volume of which is almost 5 times higher than the average volume of nanocrystallites in $ZnGa_2O_4$:Mn thin films. The volume growth is due to both the increase in the size of nanocrystallites perpendicular to the film surface and the growth of nanocrystallites in the film plane. In particular, the root mean square roughness of $ZnGa_2O_4$:Cr films is almost 3 times higher than the root mean square roughness of $ZnGa_2O_4$:Mn films, and the average grain diameter, respectively, is almost 2 times higher than the average grain diameter in $ZnGa_2O_4$:Mn films.

The characteristic optical transmission spectra $T(\lambda)$ of freshly deposited $ZnGa_2O_4$:Cr and $ZnGa_2O_4$:Mn thin films are shown in Fig. 2.

According to the results obtained, films of both types have similar transmission spectra and the edge absorption region is observed

TABLE 1. Parameters of crystalline grains on the surface of $ZnGa_2O_4$ thin films activated with Cr^{3+} and Mn^{2+} ions.

Parameter	$ZnGa_2O_4$:Cr^{3+} thin film	$ZnGa_2O_4$:Mn^{2+} thin film
RMS roughness, nm	9.6	3.9
Average grain diameter, nm	211	113
Average grain volume, nm^3	67600	11400

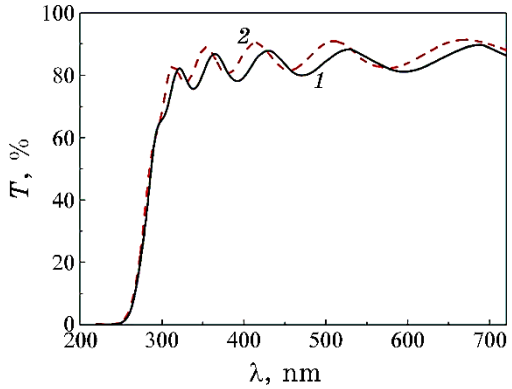

Fig. 2. Transmittance spectra of $ZnGa_2O_4$:Cr (*1*) and $ZnGa_2O_4$:Mn (*2*) thin films; $T = 295$ K.

at 260 nm. At the same time, a slight increase in light transmission is observed in $ZnGa_2O_4$:Mn films. Given that, the interference pattern is evident in the transmission spectra for both types of films, we calculated the optical constants of the films using the interference technique [13].

The obtained dispersion dependences of the refractive index $n(\lambda)$ for the studied films are shown in Fig. 3.

As can be seen in Fig. 3, both types of thin films obtained are characterized by a normal dispersion of the refractive index. To describe such dispersion dependence, we used a single oscillatory three-parameter model of the Zelmeyer type [14], which is used to describe normal dispersion:

$$\frac{n_0^2 - 1}{n^2 - A} = 1 - \left(\frac{\lambda_0}{\lambda}\right)^2. \quad (1)$$

In relation (1), the value λ_0 determines the characteristic wavelength of ultraviolet absorption or the average wavelength between the oscillator bands. This characteristic absorption is typical for most semiconductor and dielectric materials and thin films [14–17]. The value A is the approximation factor, and n_0 is the static refrac-

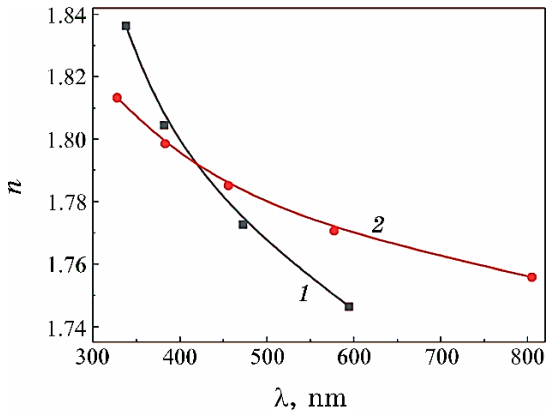

Fig. 3. Refractive index dispersion of $ZnGa_2O_4$:Cr (*1*) and $ZnGa_2O_4$:Mn (*2*) thin films.

TABLE 2. Energy parameters of the dispersion curve of freshly deposited thin films in relation (1) and (2).

Thin film	A	n_0	λ_0, nm	E_0, eV	$h\nu_p$, eV
$ZnGa_2O_4:Cr^{3+}$	2.35	1.41	250	4.96	4.93
$ZnGa_2O_4:Mn^{2+}$	2.48	1.38	260	4.78	4.58

tive index, which gives some idea of the structure and density of the material. The values of n_0 and λ_0 are determined by the dependence $(n^2 - A)^{-1}$ on λ^{-2}. The obtained values of A, n_0, λ_0, and the oscillator energy E_0, which was determined from λ_0, are shown in Table 2.

The difference of the coefficient A from 1 in relation (1) indicates the presence of other absorption bands besides the band with a maximum of E_0, which determines the course of the dispersion dependence. Such bands can be observed in both the UV and IR spectral ranges. At the same time, such additional absorption bands are more characteristic of $ZnGa_2O_4$:Mn thin films.

Previous studies have shown that the band gap in $ZnGa_2O_4$ is about 4.4 eV [18, 19]. At the same time, according to the calculations of the electronic structure of $ZnGa_2O_4$ [20, 21], the bottom of the conduction band is formed by hybridized $4s4p$ states of Zn and $4s4p$ states of Ga. The top of the valence band is formed by $2p$ oxygen orbitals and $3d$ zinc orbitals.

Taking into account our E_0 values for the obtained thin films, it can be argued that the dispersion dependence in the visible region of the spectrum of $ZnGa_2O_4$ thin films activated by Cr and Mn impurities is mainly determined by electronic transitions from the zone of $2p$-states of O and $3d$-states of Zn, which form the upper filled level of the valence band, to the bottom of the conduction band formed by hybridized $4s4p$-states of Zn and $4s4p$-states of Ga with impurities of electronic levels Cr^{3+} and Mn^{2+}, respectively.

According to Ref. [22], the average value of the oscillator energy E_0 is related to the static refractive index n_0 by the relation

$$n_0^2 \approx 1 + \frac{(h\nu_p)^2}{E_0^2}, \qquad (2)$$

where $h\nu_p$ is the energy of plasma oscillations for valence electrons. As can be seen from expression (2), there is an inversely proportional relationship between the static refractive index and the average oscillator energy and a directly proportional relationship between the static refractive index and the plasma oscillation energy.

The determined characteristic values of $h\nu_p$ for the obtained thin films are given in Table 2. Comparison of the E_0 and $h\nu_p$ values shows that in $ZnGa_2O_4$:Cr thin films these values are quite close to each other. For $ZnGa_2O_4$:Mn films, a slightly larger discrepancy is observed, which may be due to a disorder or defect in the structure. In particular, given that thin $ZnGa_2O_4$:Mn films are formed from smaller nanocrystalline grains, it is clear that they are characterized by greater imperfection due to a larger number of grain boundaries.

4. CONCLUSIONS

The studies show that polycrystalline thin films of $ZnGa_2O_4$:Cr and $ZnGa_2O_4$:Mn are obtained by RF ion-plasma sputtering in an argon atmosphere. At the same time, $ZnGa_2O_4$:Cr films are formed from significantly larger crystallites than $ZnGa_2O_4$:Mn films. In particular, the average grain diameter on the surface of the $ZnGa_2O_4$:Cr film is 211 nm, and the root mean square roughness of the films is 9.6 nm. For $ZnGa_2O_4$:Mn films, these values are 113 nm and 3.9 nm, respectively.

It was found that both types of films are characterized by a normal dispersion of the refractive index, which is determined mainly by transitions from the zone of $2p$ states of O and $3d$ states of Zn, which form the upper filled level of the valence band, to the bottom of the conduction band formed by hybridized $4s4p$ states of Zn and $4s4p$ states of Ga with impurities of electronic levels of Cr^{3+} or Mn^{2+} ions, respectively. The energy parameters of the approximation single-oscillator three-parameter model of normal dispersion dependence, which is typical for these films, are analysed.

REFERENCES

1. Mu-I Chen, Anoop Kumar Singh, Jung-Lung Chiang, Ray-Hua Horng, and Dong-Sing Wu, *Nanomaterials*, **10**, Iss. 11: 2208 (2020); https://doi.org/10.3390/nano10112208
2. G. Anoop, K. Mini Krishna, and M. K Jayaraj, *J. Electrochem. Soc.*, **158**, No. 8: J269 (2011); https://doi.org/10.1149/1.3604755
3. Chengling Lu, Qingyi Zhang, Shan Li, Zuyong Yan, Zeng Liu, Peigang Li, and Weihua Tang, *J. Phys. D: Appl. Phys.*, **54**, No. 40: 405107 (2021); https://doi.org/10.1088/1361-6463/ac1465
4. Chia-Hsun Chen, Shu-Bai Liu, and Sheng-Po Changu, *ACS Omega*, **9**, Iss. 13: 15304 (2024); https://doi.org/10.1021/acsomega.3c09965
5. Yong Eui Lee, David P. Norton, John D. Budai, Philip D. Rack, Jeff Peterson, and Michael D. Potter, *J. Appl. Phys.*, **91**, No. 5: 2974 (2002); https://doi.org/10.1063/1.1448863
6. O. M. Bordun, V. G. Bihday, and I. Yo. Kukharskyy, *J. Appl. Spectrosc.*, **80**, No. 5: 721 (2013); https://doi.org/10.1007/s10812-013-9832-2
7. Ray-Hua Horng, Shu-Hsien Lin, Yi-Che Chen, Dun-Ru Hung, Po-Hsiang Chao, Pin-Kuei Fu, Cheng-Hsu Chen, Yi-Che Chen, Jhih-Hong Shao, Chiung-Yi Huang, Fu-Gow Tarntair, Po-Liang Liu, and Ching-Lien Hsiao, *Nanomaterials*, **12**, Iss 21: 3759 (2022); https://doi.org/10.3390/nano12213759
8. O. M. Bordun, V. G. Bihday, and I. Yo. Kukharskyy, *J. Appl. Spectrosc.*, **81**, No. 1: 43 (2014); https://doi.org/10.1007/s10812-014-9884-y
9. V. Castaing, M. Romero, D. Rytz, G. Lozano, and H. Míguez, *Adv. Optical Mater.*, **12**, No. 36: 2401638 (2024); https://doi.org/10.1002/adom.202401638
10. W.-L. Huang, C.-H. Li, S.-P. Chang, and S.-J. Chang, *ECS J. Solid State*

Sci. Technol., **8**, No. 7: Q3213 (2019); https://doi.org/10.1149/2.0371907jss
11. Kiyotaka Wasa, Makoto Kitabatake, and Hideaki Adachi, *Thin Film Materials Technology: Sputtering of Compound Materials* (New York: Springer–William Andrew Inc. Publishing: 2004).
12. O. M. Bordun, I. O. Bordun and I. Yo. Kukharskyy, *J. Appl. Spectrosc.*, **78**, No. 6: 922 (2012); https://doi.org/10.1007/s10812-012-9555-9
13. R. Swanepoel, *J. Phys. E: Sci. Instrum.*, **16**, No. 12: 1214 (1983); https://doi.org/1010.1088/0022-3735/16/12/023
14. M. Abdel-Baki, F. A. Abdel Wahab, and F. El-Diasty, *Mater. Chem. Phys.*, **96**, Nos. 2–3: 201 (2006); https://doi.org/10.1016/j.matchemphys.2005.07.022
15. S. H. Wemple and M. Di Domenico, *Phys. Rev. B*, **3**: 1338 (1971); https://doi.org/10.1103/PhysRevB.3.1338
16. O. M. Bordun, I. Yo. Kukharskyy, B. O. Bordun, and V. B. Lushchanets, *J. Appl. Spectrosc.*, **81**, No. 5: 771 (2014); https://doi.org/10.1007/s10812-014-0004-9
17. O. M. Bordun, I. Yo. Kukharskyy, and I. I. Medvid, *J. Appl. Spectrosc.*, **83**, No. 1: 141 (2016); https://doi.org/10.1007/s10812-016-0257-6
18. M. Nonaka, T. Tanizaki, S. Matsushima, M. Mizuno, and C.-N. Xu, *Chem. Lett.*, **30**, No. 6: 664 (2001); https://doi.org/10.1246/cl.2001.664
19. S. K. Sampath and J. F. Cordaro, *J. Am. Ceram. Soc.*, **81**, No. 3: 649 (1998); https://doi.org/10.1111/j.1151-2916.1998.tb02385.x
20. K. Ikarashi, J. Sato, H. Kobayashi, N. Saito, H. Nishiyama, and Y. Inoue, *J. Phys. Chem. B*, **106**, No. 35: 9048 (2002); https://doi.org/10.1021/jp020539e
21. Suresh K. Sampath, D. G. Kanhere, and Ravindra Pandey, *J. Phys.: Condens. Matter*, **11**: 3635 (1999); https://doi.org/10.1088/0953-8984/11/18/301
22. David R. Penn, *Phys. Rev.*, **128**: 2093 (1962); https://doi.org/10.1103/PhysRev.128.2093